simplify the analysis, although it may be interesting to consider the general situation.

ACKNOWLEDGMENTS

This paper presents results of one phase of research carried out at the Jet Propulsion Laboratory, California Institute of Technology, under Contract No. NAS7-100, sponsored by the National Aeronautics and Space Administration. The authors want to thank Mrs. Sayuri Harami for her capable assistance in numerical computation.

[1]Yu. L. Klimontovich, Statistical Theory of Non-Equilibrium Processes in a Plasma (Massachusetts Institute of Technology Press, Cambridge, Mass., 1967)

[2]N. Rostoker, Nucl. Fusion 1, 101 (1960).

[3]L. M. Gorbunov and V. P. Silin, Zh. Tekhn. Fiz. 34, 385 (1964) [English transl.: Soviet Phys. – Tech. Phys. 9, 305 (1964)].

[4]C. S. Wu, E. H. Klevans, and J. R. Primack, Phys. Fluids 8, 1126 (1965).

[5]D. A. Tidman and A. Eviatar, Phys. Fluids 8, 2059 (1965).

[6]D. A. Tidman and T. H. Dupree, Phys. Fluids, 8, 1860 (1965).

[7]"Degenerate" means that the frequency of the wave is much lower than the ion cyclotron frequency and that its propagation characteristics are different from those of the usual ion acoustic wave. Further discussion of this wave will be given in Sec. III, A.

[8]Anisotropy does not play a major role in our analysis; it is assumed here mainly for the sake of generality.

[9]We are considering a situation in which electrons and ions are initially at the same temperature and subsequentially the electron temperature is increased, while the ion temperature is held fixed.

PHYSICAL REVIEW VOLUME 177, NUMBER 1 5 JANUARY 1969

Trapping Lifetime of Negative Ions in Rotating Superfluid Helium Under Pressure

W. P. Pratt, Jr.,* and W. Zimmermann, Jr.

Tate Laboratory of Physics, University of Minnesota, Minneapolis, Minnesota

(Received 26 August 1968)

Measurements have been made of the lifetime for the escape of negative ions trapped in rotating helium II as a function of temperature and pressure. These measurements concern lifetimes in the range from 10 to 1000 sec, and have been made between the temperatures of 1.09 and 1.68°K from the vaporization pressure to the solidification pressure. At constant pressure the lifetime decreases rapidly with increasing temperature. The curves of constant lifetime in the pressure-versus-temperature plane have negative slopes dP/dT and positive second derivatives d^2P/dT^2. The results have been interpreted in terms of the bubble model of the negative ion and the vortex-line model of the rotating superfluid. The interpretation suggests that the ion radius equals approximately 19.5 A at saturated vapor pressure and decreases to a value between 12 and 14 Å at the solidification pressure. However, a significant discrepancy between theory and experiment casts some doubt on the radius values obtained.

I. INTRODUCTION

A number of recent experiments have shown that when negative ions are made to cross a steadily rotating vessel containing liquid helium II, in a direction perpendicular to the axis of rotation, some of the ions can become trapped in the liquid.[1-3] At saturated vapor pressure the trapping becomes significant below about 1.7°K. At this pressure Tanner, Springett, and Donnelly[4,5] and Douglass[6] have studied the absorption of ions from a beam, and Douglass[3] has made measurements of the lifetime for the escape of ions trapped in the liquid. As the pressure is increased the temperature below which trapping is significant decreases. The capture process at elevated pressures has recently been studied by Springett and Donnelly.[7,8] In the present work we have made direct measurements of the lifetime for escape both at saturated vapor pressure and also at elevated pressures.[9] Thus our measurements complement and extend the other measurements referred to above.

The ion trapping has been interpreted in terms of the bubble model of the negative ion and the vortex-line model of the rotating superfluid.[10,11] In accord with these models, the superfluid is considered to rotate in imitation of solid-body

motion by virtue of the formation of a uniform array of rectilinear vortices lying parallel to the axis of rotation. An attractive interaction is thought to exist between an ion and a vortex owing to hydrodynamic effects. As a result, the vortices provide an array of linear potential wells in which the ions may become trapped. The trapping is thought to be limited only by thermally activated escape of the ions in the radial direction and by migration of the ions along the vortices to their ends. Interpreted in this way, experiments on the trapping of negative ions lead to a combination of information about the negative ion and superfluid vortices. In the present work we have been particularly interested in estimating the radius of the negative ion and its dependence upon pressure.

II. EXPERIMENTAL APPARATUS

The cell in which the ion trapping was studied is illustrated in Fig. 1. During measurements the cell was filled with liquid helium which could be maintained at any pressure between the vaporization and solidification pressures. The cell was completely surrounded by an outer liquid-helium bath which could be pumped down to a lowest temperature of about 1.09°K. The cell was rotationally symmetric about a vertical axis and was suspended from a turntable at the top of the cryostat so that it could be put into steady rotation.

The electrodes in the ion trapping cell were made of No. 303 stainless steel and were electropolished in a solution consisting of 60% glycerine and 40% phosphoric acid. In experiments such as these it is quite important to minimize the formation of insulating surfaces on the electrodes, in order to avoid the buildup of electrostatic charge and the subsequent distortion of

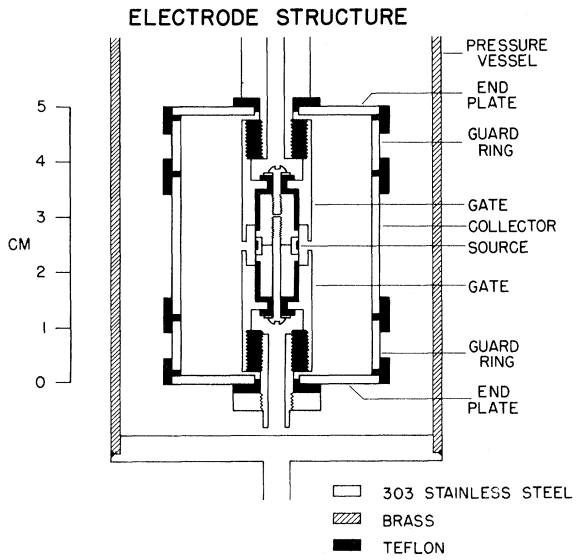

FIG. 1. Diagram of the liquid-helium-filled cell in which the ion trapping was studied. The electrode structure and pressure vessel possess rotational symmetry about a vertical axis.

the applied electric field. Although it is customary for this purpose to use electrodes that have been plated with gold, we believe that the polished stainless-steel surfaces used in the present work were entirely satisfactory in this regard. No drifts in electric-field-dependent quantities were ever observed during individual runs, and measurements of such quantities several months apart were quite reproducible. Care was taken between experimental runs to be sure that only helium gas of high purity came into contact with the electrodes. The gate electrode had an outer radius $a = 0.64$ cm, and the collector and guard rings had an inner radius $b = 1.75$ cm. The electrodes were separated by Teflon insulators.

The ion source consisted of small glass beads 40 μ in size into which a small quantity of the α emitter Po^{210} had been sealed.[12] These beads were glued into a groove on the surface of a ring-shaped source electrode and were covered with a vacuum-deposited layer of gold approximately 2000 Å thick. The source activity was initially about 100 μCi and during the course of the measurements decreased to about 10 μCi.

The collector lead was brought out of the pressure vessel by means of a commercial porcelain superleak-tight feedthrough.[13] The other electrical leads were brought out using seals made with an epoxy polymer.[14]

The cell was supported from the turntable by three thin-wall stainless-steel tubes each having a diameter of 2.5 cm. One of these tubes contained a coaxial thin-wall stainless-steel tube 0.5 cm in diameter supported every 12.5 cm by Teflon plugs. This tube served as a mechanically stable, well-insulated, low-capacitance connection between the collector electrode and the input to an electrometer mounted on the turntable. The electrometer was of the vacuum-tube-input type and had a response time of about $\frac{1}{2}$ sec.

The turntable was supported by a 12-cm-diameter ball bearing, and a rotating vacuum seal was made between turntable and Dewar using a commercial oil seal.[15] The turntable could be put into steady rotation at speeds up to about 11 rad sec^{-1} using a synchronous motor and variable-speed transmission unit mounted with some degree of vibration isolation on the Dewar stand.[16]

External connections to the electrode leads and to the electrometer output were made through a rotating mercury-trough connector. In this way electrode potentials could be set and the collector current measured in rotation as well as at rest. The electrometer output was connected to a chart recorder in order to display the collector current as a function of time. The electrometer output was also connected to an integrating circuit. The output of this circuit was in turn connected to another chart recorder to display the total charge collected as a function of time.

The cell was provided with a valve which could be operated from the top of the cryostat so that the cell could be filled with liquid helium at low pressure directly from the bath. Further filling and pressurization were carried out by condensation of helium gas through a stainless-steel

capillary. This capillary had an inner diameter of about 0.25 mm and connected the cell to a pressure manifold mounted on the turntable. The manifold was in turn connected to an external helium-gas supply through a rotating connector which allowed pressure measurements to be made in rotation on a stationary gauge. Helium gas supplied to the system was purified by being passed through a liquid-nitrogen–cooled trap containing activated charcoal.

Pressure measurements at low pressures were made using two mercury manometers in series. In the intermediate range a 0- to 200-lb in.$^{-2}$ Bourdon gauge rated at an accuracy of $\pm\frac{1}{4}\%$ of its full scale value was used.[17] For higher pressures a 0- to 600-lb in.$^{-2}$ gauge of the same type rated at the same percentage accuracy was used. No attempt was made to calibrate these gauges against an accurate standard. However, the 200- and 600-lb in.$^{-2}$ gauges agreed within their stated accuracies.

The temperature of the bath surrounding the cell was electrically regulated to better than $\pm 5 \times 10^{-5}$ °K. The regulator was similar in principal to one described by Blake and Chase[18] and made use of a germanium resistance thermometer[19] and an electrical bath heater. The bath temperature was measured in terms of the 1958 He^4 vapor-pressure scale of temperatures[20] using a 1.3-cm-bore manometer containing Octoil-S.[21] The density of the oil was determined at various room temperatures by using the manometer to measure the vapor pressure of He^4 at the lambda point, where the vapor pressure was taken to be 37.80 mm of mercury.

In order to avoid errors at the lowest temperatures due to a pressure drop between the liquid surface and the top of the Dewar associated with the gas flow from the evaporating liquid, vapor-pressure measurements were made using a separate thin-wall stainless-steel tube 1.0 cm in diameter extending down into the Dewar. Pressure measurements made in this way were corrected for a significant thermomolecular pressure drop at the lowest temperatures using the data given by Roberts and Sydoriak.[22] It is believed that the accuracy to which bath temperatures were determined on the 1958 He^4 scale varied from about $\pm 1\times10^{-4}$ °K at 1.7°K to $\pm 5\times10^{-4}$ °K at 1.1°K.

We have assumed that the temperature of the liquid inside the cell was sufficiently close to that of the bath for any difference to have been negligible. The bath completely covered the cell and surrounded all connections between the cell and room temperature, and the only source of heat within the cell was the radioactive source. At the initial source strength of 100 μCi the heating is estimated to have been about 3 μW, an amount of power which is estimated to be too small to have had a detectable effect on the temperature inside the cell.

The potentials of the electrodes were set as follows. The electrometer to which the collector was connected was arranged in such a way that for the collector currents measured in the present experiment the collector remained within a millivolt of ground potential. The guard rings were grounded. For negative-ion measurements the gate potential was generally chosen to be -40 V, the potential of the end plates to be -80 V, and the potential difference between the source and gate to be ∓ 57 V depending on whether the ion current was to be turned on or off.

On some occasions, when the electric-field dependence of the lifetime was being investigated, different values of the gate potential were used. On these occasions the other potentials were scaled accordingly so that the field configuration within the electrode structure remained the same. During a search for positive-ion trapping all the potentials were reversed. The electrode potentials were measured to an accuracy of about $\pm 1\%$.

The end-plate potential was chosen in relation to the gate potential to provide a confining field component in the vertical direction, in order to keep trapped charge from leaking out the ends of vortex lines. Detailed calculations of the field configuration in the region between the collector and gate were made to determine the effectiveness of the confining potential. With space charge present the confinement effect tends to be reduced by the self-field of the charge. However, estimates indicated that with the usual potentials the applied fields were ample to confine the largest amounts of charge trapped, approximately 5×10^{-12} C, except possibly in small regions very close to the gate and collector electrodes. On the other hand, these estimates suggested that when the gate potential was of the order of -1 V, the smallest value used, the confinement was marginal, even with the smaller amounts of trapped charge used in this case. Nevertheless, no effects associated with charge leakage were noticed, even at low gate potentials.

The source-to-gate potential difference was chosen in relation to the gate potential so that when the ion current was on, the equipotential surfaces between the gate and collector would be as little distorted from a cylindrical shape as possible near the gap in the gate electrode. A mockup of the electrode system in an electrolytic tank was used for this determination. The current transmitted by the gate under these circumstances was about 25% of the source-to-gate current. Collector currents of the order of 10^{-13} to 10^{-12} A were typical.

III. PROCEDURE FOR THE DETERMINATION OF TRAPPING LIFETIMES AND SOME RELATED EXPERIMENTAL OBSERVATIONS

A. Procedure

The following phenomenon formed the basis of our procedure for measuring the trapping lifetime of negative ions in the rotating liquid. If first some negative charge had been trapped in the rotating liquid with the electrode potentials set as described in the preceding section, it was observed that when the rotation was suddenly stopped, a pulse of current would flow through the electrometer. The charge contained in this pulse was of the cor-

rect order of magnitude to represent the release of the charge held in the liquid. Although we have no clear picture of the mechanism involved in the release, we have assumed in our lifetime measurements that the charge contained in these current pulses gave a suitable measure of the amount of charge held in the liquid just before rotation was stopped.

To measure the lifetime at a given temperature and pressure, the first step was to trap a reproducible amount of charge in the liquid. This step was accomplished by rotating the cell for 360 sec with the negative-ion current on. The usual rotation speed was 6.3 rad sec^{-1}. At this speed a rotation period of 360 sec appeared to be long enough for the establishment of a stable state of rotation in the liquid with enough charge present to make lifetime measurements possible. However, the liquid was not generally charged to saturation.

At the end of this period the ion current was turned off by reversal of the electric field between the source and gate electrodes. After a variable waiting period t the rotation was suddenly stopped, the deceleration taking approximately $\frac{1}{2}$ sec. The current pulse received by the electrometer was then recorded and the total charge measured using the integrating circuit. We have designated this current and its integral as the apparent ion current and the apparent trapped charge, respectively.

The recordings of apparent ion current shown in Fig. 2 illustrate the events during such a measurement cycle. Figure 2(a) shows the apparent ion current during a cycle at the usual rotation speed. Figure 2(b) differs from 2(a) only in that the rotation speed is higher. Figures 2(c) and 2(d) show on an expanded time scale the details of the current pulse after the rotation was stopped for the two different speeds of rotation.

At each temperature and pressure the procedure above was repeated several times with waiting periods of different length. It was observed that the charge in the final pulse depended exponentially on t in proportion to $e^{-t/\tau}$, where the quantity τ was independent of t but depended on temperature and pressure. It is this quantity τ which we define to be the trapping lifetime. In each case measurements were performed out to a waiting period of length 2τ. It is estimated that typically the lifetimes were determined with an accuracy which varied from about ± 5% for a lifetime of 10 sec to about ± 2% for a lifetime of 1000 sec.

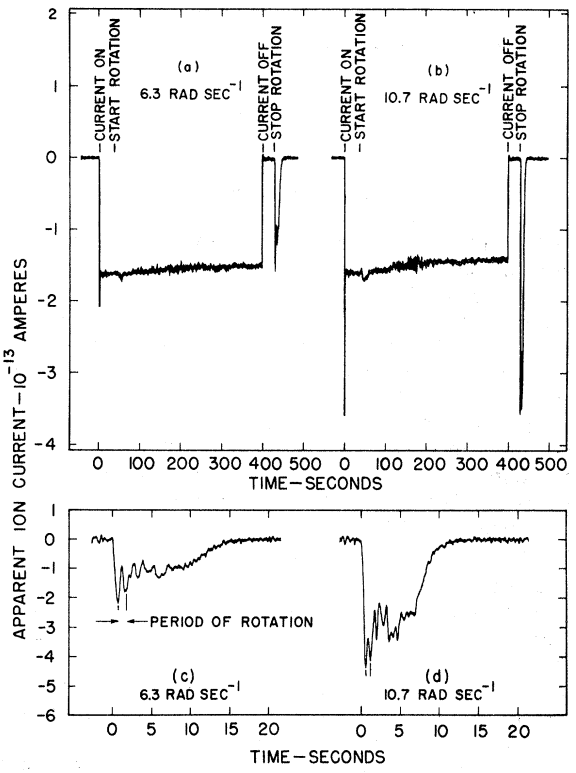

FIG. 2. Sample recordings of the apparent ion current versus time made at 1.59°K and saturated vapor pressure with $V_g = -40$ V. The trapping lifetime was 920 sec. Traces (a) and (b) show the current during two measurement cycles which differed only in regard to the speed of rotation. The waiting periods t in these cycles were 30 sec. Traces (c) and (d) were taken with a faster recorder under the same conditions as (a) and (b), respectively, and show the details of the final current pulses occurring after rotation was stopped.

B. Comments on the Procedure

In regard to the period during which the liquid is being charged after the cell has been set in rotation, there are two characteristic times to be considered. The first is the time required for a stable rotational state of the liquid to be established; the second is the time required for an equilibrium charge density to be attained. For lifetime measurements it may be important for the charging time to be longer than the first of these times, since changes in the rotational state which occur during the waiting period could conceivably lead to erroneous lifetime values. On the other hand, the length of the charging time in relation to the second characteristic time is probably not of importance as long as the charge density is ultimately limited by escape of the ions in the radial direction rather than by leakage out the ends of the vortex lines.

Unfortunately, our evidence that a stable rotational state was established within the 360-sec charging period is not as strong as could be desired. However, some observations of the rate of charge buildup in the liquid as a function of time after start of rotation suggest that about 180 sec were sufficient for an equilibrium rotational state to be established at 6.3 rad sec^{-1}.

It is worth noting that, owing to the fact that the negative charge trapped in the liquid induces positive charge on the collector electrode, the charge flowing through the electrometer upon release of charge by the liquid is only some fraction of the ionic charge actually reaching the collector. It is for this reason that we have called the current flowing through the electrometer and its integral the apparent ion current and apparent trapped charge, respectively. The ratio of the apparent to the actual quantities here should depend only on the distribution of trapped charge just before re-

lease. For a uniform distribution the ratio was estimated to equal 0.34.

C. Related Observations

Several interesting effects were noted in relation to the release of charge by the liquid upon sudden stop. The early part of the pulse of apparent ion current generally showed a series of equally spaced peaks whose separation equalled the period of rotation that had existed just before stopping. Despite the rotational symmetry of the geometry these peaks must in some way have reflected the tendency of the liquid to coast at the same rate after the walls had stopped as when the walls were in motion. In addition, the length of the entire pulse was a function of rotation speed, growing shorter as the speed was increased. Illustrations of both these effects may be seen in the lower parts of Fig. 2.

Some additional observations were made under the same conditions as apply to Fig. 2. If 5 sec after the original rotation at 6.3 rad sec^{-1} was stopped the cell was suddenly put into reverse rotation at 6.3 rad sec^{-1}, the charge remaining in the liquid was observed to be released in 2 to 3 sec, a considerably shorter time than the 15 sec or so that would have been required if the cell had remained at rest. If 5 sec after rotation at 6.3 rad sec^{-1} was stopped forward rotation at the same speed was restarted, the current pulse being recorded was immediately reduced; and a second stop in rotation 70 sec later revealed that charge still remained in the liquid.

Some observations of the apparent ion-current pulse were made in which the electric field between gate and collector was reversed at the end of the charging period. In this case the current pulse was reversed in sign relative to the usual case, indicating that the ions were being collected by the gate. The magnitude of the apparent charge in the pulse with a reversed field was 1.7 times the magnitude with the usual field direction, in rough agreement with the ratio of 1.9 expected for a uniform distribution of trapped charge. Strangely enough, however, the pulse length was over two times longer than that for the normal field direction.

Measurements of the apparent amount of charge trapped in the liquid as a function of speed of rotation were made at 1.635°K and saturated vapor pressure. The measurements involved the usual 360-sec charging period followed by a 10-sec waiting period before stopping rotation. Because for rotation speeds of less than about 2 rad sec^{-1} the pulse became long enough for appreciable error to result from electrometer drift during integration, the measurements at these speeds involved a reversal of rotation after stopping in order to shorten the release time for the trapped charge. The results are shown as solid circles in Fig. 3. It can be seen that the relationship is quite linear in the region studied.

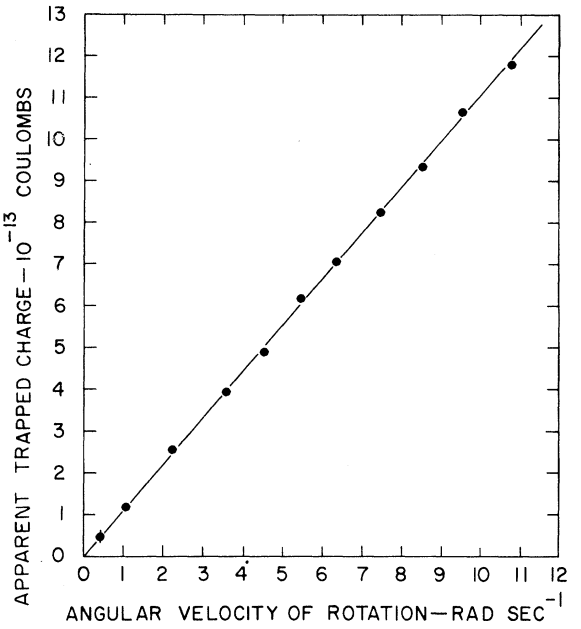

FIG. 3. Apparent trapped charge versus angular velocity of rotation measured at 1.635°K and saturated vapor pressure with $V_g = -40$ V. The trapping lifetime at $\omega = 6.3$ rad sec^{-1} was 105 sec.

TABLE I. Trapping-lifetime measurements at saturated vapor pressure with $\omega = 6.3$ rad sec^{-1}.

V_g (V)	T (°K)	τ (sec)
−1.0	1.6490	148 ± 8
−5.0	1.6490	98 ± 3
	1.6355	187 ± 5
−10	1.6490	81 ± 2
	1.6355	157 ± 3
−20	1.6792	16.1 ± 1.0
	1.6592	42 ± 1
	1.6398	107 ± 5
	1.6239	230 ± 5
	1.6074	485 ± 10
−40	1.6796	11.1 ± 0.4
	1.6785	10.8 ± 0.7
	1.6715	17.5 ± 0.7
	1.6659	22.8 ± 0.6
	1.6610	29.5 ± 0.8
	1.6602	31.0 ± 0.7
	1.6545	39.5 ± 0.8
	1.6489	52.5 ± 1.0
	1.6455	62.2 ± 1.5
	1.6350	105 ± 2
	1.6347	103 ± 3
	1.6286	143 ± 4
	1.6130	300 ± 5
	1.6044	455 ± 5
	1.5977	625 ± 20
	1.5897	920 ± 20
−80	1.6715	11.4 ± 0.5
	1.6528	31.3 ± 1.0
	1.6355	71 ± 1
	1.6314	90 ± 2
	1.6170	167 ± 3
	1.5963	470 ± 10

IV. TRAPPING-LIFETIME RESULTS

A. Trapping Lifetime at Saturated Vapor Pressure

At saturated vapor pressure the trapping lifetime was measured as a function of temperature for several values of the gate potential V_g. The results are listed in Table I and presented graphically in Fig. 4. It can be seen from Fig. 4 that for each value of V_g a plot of $\ln\tau$ versus $1/T$ is very nearly a straight line with a slope that is rather independent of V_g.

The electric-field dependence of the lifetime is shown in another manner in Fig. 5, where the solid circles represent the logarithm of the lifetime at 1.65°K plotted versus the average electric field $\mathcal{E}_{av}$ between the gate and collector electrodes. Here $\mathcal{E}_{av}$ is defined as the average of the magnitude of the electric field over the cross-sectional area lying between the gate and collector electrodes. It is given by the relation

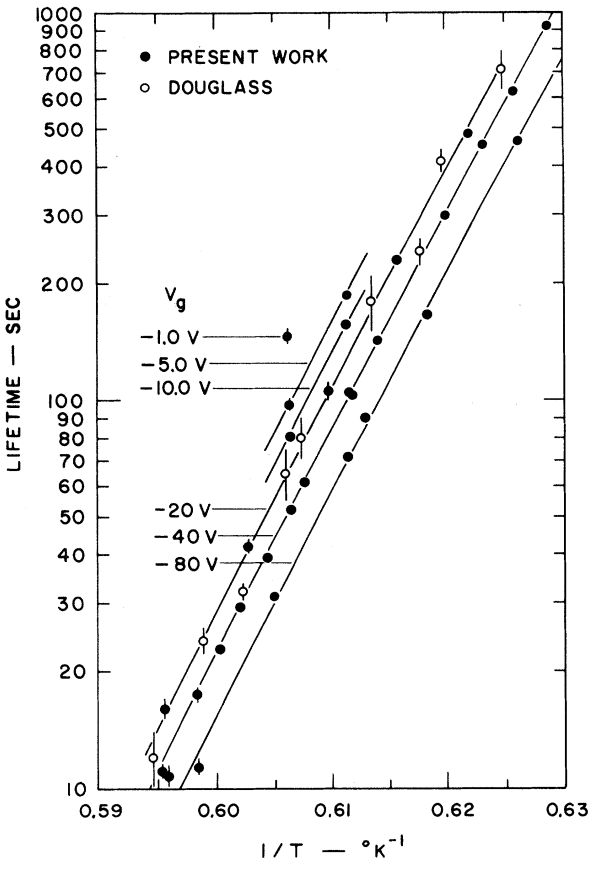

FIG. 4. Logarithm of the trapping lifetime versus $1/T$ at saturated vapor pressure. Solid circles show our results at several values of the gate potential with $\omega = 6.3$ rad sec^{-1}. Open circles show the results of Douglass. Curve through the $V_g = -40$ V points is a computer-calculated fit to these points discussed in Sec. VI B. Other curves are merely parallel displacements of this first curve in the vertical direction.

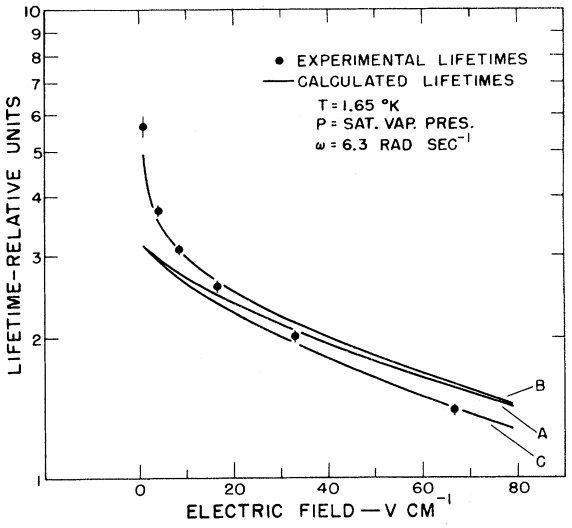

FIG. 5. Logarithm of the trapping lifetime in relative units versus electric field at 1.65°K and saturated vapor pressure. Solid circles show our experimental results plotted against the average electric field in the cell $\mathcal{E}_{av}$. Curves A, B, and C show the calculated field dependences of τ discussed in Sec. VI, B.

$$\mathcal{E}_{av} = 2|V_g|/(a+b)\ln(b/a),$$

where a and b are, respectively, the outer radius of the gate electrode and the inner radius of the collector. In the present case we have $\mathcal{E}_{av} = 0.83|V_g|$, which for $V_g = -40$ V gives $\mathcal{E}_{av} = 33.2$ V cm^{-1}. The actual applied electric field varied in magnitude from 1.88 $\mathcal{E}_{av}$ at the gate to 0.68 $\mathcal{E}_{av}$ at the collector.

A check was made to see whether the lifetime measured was dependent on the angular velocity of rotation. A small effect was observed, the lifetime at 1.635°K varying from 102 ± 2 sec at a rotation speed of 3.5 rad sec^{-1} to 107 ± 3 sec at 10.7 rad sec^{-1} with $V_g = -40$ V.

Also plotted in Fig. 4 are the lifetime results of Douglass, which were measured by a somewhat different technique in rotationally symmetric geometry with a computed $\mathcal{E}_{av}$ of 22.7 V cm^{-1}.[3,23] The slope of $\ln\tau$ versus $1/T$ given by his data seems to be in very good agreement with our slopes. The magnitudes appear to be in reasonable agreement, taking the field dependence of the lifetime into account. In view of the fact that in Douglass's experiment the trapped charge remaining in the liquid was extracted in a direction parallel to the axis of rotation with the container still rotating, the agreement between his results and ours at saturated vapor pressure helps to support the validity of our sudden-stop method of extracting the charge for the purpose of lifetime measurement.

B. Trapping Lifetime at Elevated Pressure

Lifetime measurements were made at 15 values

of the pressure between the vaporization and solidification pressures and also along the solidification curve itself. At each value of the pressure, lifetimes were measured in the range from about 20 to 500 sec at several different temperatures. The results are listed in Table II. For all of these measurements a gate potential of -40 V and a rotation speed of 6.3 rad sec^{-1} were used. At the highest pressures the range of measurement was unfortunately limited by the lowest temperature we could reach, 1.094°K.

At each value of the pressure $\ln\tau$ was plotted against $1/T$. It was found that in most cases the data fell along straight lines, as they did at saturated vapor pressure to good approximation. The slopes of these plots are listed in Table II and shown plotted against pressure in Fig. 6. Interpolation of the data, which was made easy by the linearity of these plots, was then used to construct curves of constant lifetime in the pressure-versus-temperature plane. Three such curves were constructed, for lifetimes of 20, 85, and 350 sec. These curves are shown in Fig. 7, and the coordinates of the points used to construct them are listed in Table III.

Also plotted in Fig. 7 are some points derived from the capture-width measurements of Springett and Donnelly.[7,8] Each point represents at its respective pressure the temperature at which the apparent capture width has fallen to one half the value of the intrinsic capture width determined by extrapolation from temperatures below the maximum. According to the interpretation of Springett and Donnelly, the locus of these points is given by the relation $t_m = 0.69\tau$, where t_m is the time required for captured ions to migrate along the vortex lines out of the active region of their experimental cell. The fact that this locus very nearly coincides with one of our curves of constant lifetime implies that t_m was rather independent of pressure in their experiment and thus supports one of the assumptions they consider in their determinations of the ion radius as a function of pressure.

It should be pointed out that the measurements at the solidification pressure were actually made along the phase boundary, with about 2 or 3% of the cell volume occupied by solid helium. Since the transition is of the first order, there is no difficulty in holding the system at the transition.

Along with measurements of the negative-ion

TABLE II. Trapping-lifetime measurements at elevated pressure with $V_g = -40$ V and $\omega = 6.3$ rad sec^{-1}.

P (atm)	T (°K)	τ (sec)	$d(\ln\tau)/d(1/T)$ (°K)
0.997 ± 0.002	1.5992	27.5 ± 1.0	116 ± 1
	1.5795	71 ± 1	
	1.5595	182 ± 4	
	1.5390	470 ± 9	
1.995 ± 0.002	1.5595	20.5 ± 1.0	107 ± 1
	1.5390	51.0 ± 1.0	
	1.5203	122 ± 3	
	1.4991	330 ± 6	

TABLE II (*continued*)

P (atm)	T (°K)	τ (sec)	$d(\ln\tau)/d(1/T)$ (°K)
3.00 ± 0.03	1.5208	19.6 ± 0.8	99 ± 1
	1.4998	55 ± 2	
	1.4799	131 ± 2	
	1.4588	326 ± 3	
4.00 ± 0.03	1.4793	26 ± 1	93 ± 2
	1.4584	65 ± 1	
	1.4399	147 ± 2	
	1.4185	380 ± 7	
5.00 ± 0.03	1.4474	30.5 ± 1.0	84 ± 1
	1.4349	51 ± 3	
	1.4240	77.5 ± 1.0	
	1.4145	115 ± 2	
	1.4042	181 ± 2	
	1.3941	290 ± 5	
6.00 ± 0.03	1.4315	21 ± 1	79.5 ± 1.0
	1.4188	34.5 ± 1.0	
	1.4078	51.5 ± 1.0	
	1.3993	72 ± 2	
	1.3880	114 ± 2	
	1.3795	160 ± 3	
	1.3675	277 ± 5	
	1.3594	390 ± 5	
8.00 ± 0.03	1.3739	26 ± 2	75.5 ± 1.0
	1.3542	58 ± 2	
	1.3346	137 ± 2	
	1.3140	320 ± 5	
10.00 ± 0.03	1.3339	23.5 ± 1.0	73 ± 1
	1.3143	54 ± 2	
	1.2943	128 ± 2	
	1.2753	285 ± 5	
12.00 ± 0.03	1.2936	26.5 ± 1.0	70 ± 1
	1.2749	57.5 ± 1.0	
	1.2551	142 ± 3	
	1.2353	325 ± 5	
14.00 ± 0.03	1.2579	26.0 ± 1.0	68.5 ± 1.0
	1.2384	62.5 ± 1.0	
	1.2192	150 ± 2	
	1.2012	345 ± 7	
16.0 ± 0.1	1.2355	17.3 ± 0.5	66.5 ± 1.0
	1.2151	43 ± 1	
	1.1952	107 ± 3	
	1.1747	285 ± 5	
18.0 ± 0.1	1.1996	23.5 ± 1.0	65 ± 1
	1.1786	65 ± 2	
	1.1590	165 ± 5	
	1.1383	455 ± 10	
20.0 ± 0.1	1.1713	27 ± 1	62 ± 1
	1.1487	82 ± 4	
	1.1286	198 ± 4	
	1.1090	530 ± 10	
22.0 ± 0.1	1.1484	22 ± 1	61 ± 1
	1.1283	60.5 ± 1.0	
	1.1092	148 ± 3	
	1.0946	310 ± 6	
24.0 ± 0.1	1.1283	19.5 ± 1.0	57 ± 3
	1.1071	56 ± 2	
	1.0942	90 ± 3	
25.1 ± 0.1 (along the solidification curve)	1.1185	18.5 ± 1.0	54 ± 3
	1.1139	23.5 ± 1.0	
	1.1041	34 ± 2	
	1.0950	52 ± 1	

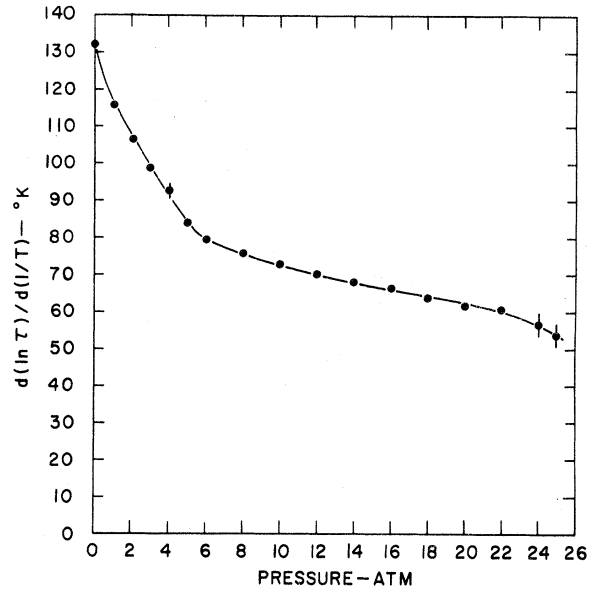

FIG. 6. The derivative $d(\ln\tau)/d(1/T)$ at constant pressure versus pressure. The solid circles show the values derived from our data. The curve is merely a smooth connection between the circles drawn by eye.

lifetime at the solidification pressure, a search was made for positive-ion trapping in the rotating liquid. None was observed within the temperature and lifetime ranges accessible to us, nor was any positive-ion trapping seen at lower pressures and higher temperatures.

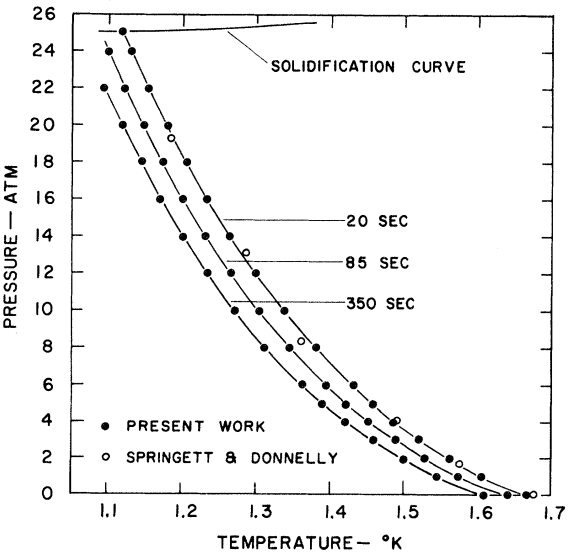

FIG. 7. Solid circles show curves of constant lifetime in the pressure versus temperature plane determined from our data. Curve segments are merely smooth connections between the circles drawn by eye. Open circles show points derived from the work of Springett and Donnelly as explained in Sec. IV, B.

TABLE III. Curves of constant lifetime in the pressure versus temperature plane with $V_g = -40$ V and $\omega = 6.3$ rad sec^{-1}.

	$\tau = 20$ sec	$\tau = 85$ sec	$\tau = 350$ sec
P (atm)	T (°K)	T (°K)	T (°K)
0.0	1.669	1.642	1.610
1.0	1.606	1.575	1.545
2.0	1.562	1.528	1.498
3.0	1.522	1.489	1.458
4.0	1.486	1.452	1.421
5.0	1.458	1.422	1.389
6.0	1.432	1.395	1.362
8.0	1.381	1.345	1.312
10.0	1.338	1.304	1.271
12.0	1.300	1.266	1.234
14.0	1.264	1.231	1.201
16.0	1.232	1.200	1.170
18.0	1.205	1.173	1.143
20.0	1.179	1.147	1.117
22.0	1.151	1.121	1.092
24.0	1.129	1.097	
25.1	1.117		

V. MODELS FOR THE RETENTION AND ESCAPE OF THE IONS

A. The Bubble Model of the Negative Ion

The idea that the negative ion in liquid helium consists of an electron contained in a small cavity devoid of helium atoms seems to have been suggested first by Careri,[24] following a similar proposal regarding positronium in liquid helium made by Ferrell.[25] This model has since been developed by a number of workers.[26-32]

It has been estimated theoretically that due to an effective repulsive interaction between a low-energy electron and a helium atom, a minimum energy of about 1.1 eV is required to place an electron in liquid helium in the absence of any rearrangement of the helium atoms.[33] This estimate has been supported experimentally by the work of Sommer[34] and of Woolf and Rayfield.[35] However, it appears to be energetically favorable for a small cavity devoid of helium atoms to form around the electron, in which the electron is effectively confined. The energy needed to form the cavity is more than compensated for by the decrease in the electron zero-point energy.

A very simple calculation to estimate the radius of the cavity and its dependence on pressure can be made in the following way. Consider the cavity to provide for the electron a spherical square well with walls of infinite height. The total energy E needed to form the cavity and to place the electron in it can then be written in the form

$$E = \pi^2\hbar^2/2m_eR^2 + 4\pi R^2\sigma + \tfrac{4}{3}\pi R^3P, \qquad (1)$$

where $\hbar$ is Planck's constant divided by 2π, m_e is the mass of the electron, R is the radius of the cavity, σ is the bulk surface tension of the liquid, and P is the pressure in the liquid. The first term

on the right is the energy needed to confine the electron to the cavity, the second term is an estimate of the energy needed to create the cavity at zero pressure, and the last term represents the additional energy needed to create the cavity when the pressure is not zero. The equilibrium radius of the ion is found by minimizing E with respect to variations in R. Using the value $\sigma = 0.373$ erg cm^{-2}, which seems to be appropriate for 0°K,[36] the equilibrium radius at $P = 0$ is found to be 18.9 Å and the corresponding total energy to be 0.21 eV. If we ignore possible changes in σ with pressure, the radius decreases with increasing pressure, reaching 12.5 Å at 25 atm.

It should be emphasized that this calculation is a very crude one. Nevertheless it serves to give a helpful picture of the basic elements involved in the model. A possible improvement of the calculation would be the inclusion of a term in the expression for E representing the energy due to electrical polarization of the helium atoms in the vicinity of the electron. At zero pressure this effect reduces the equilibrium radius from 18.9 to 18.5 Å. Another possible improvement would be to assume that the walls of the potential well have a height of 1.1 eV instead of an infinite height. At zero pressure the inclusion of this effect by itself reduces the equilibrium radius from 18.9 to 17.6 Å. However, for a more accurate picture of the ion a more complete many-body calculation is required.

It is plausible that the effective mass m_i of such an ion will be principally hydrodynamic in origin, arising from the motion imposed on the surrounding fluid by the motion of the ion. At low temperatures, where the effect of the normal fluid can be ignored, an estimate of the effective mass may be made by using the classical expression for the effective hydrodynamic mass added to a sphere moving in an ideal fluid. This added mass is given by the expression $\frac{2}{3}\pi R^3\rho$, where ρ is the density of the fluid. For an ion radius of 18.9 Å and a fluid density of 0.146 gm cm^{-3}, this expression yields an m_i of approximately $310m_4$, where m_4 is the mass of a helium atom.

B. The Vortex-Line Model of the Rotating Superfluid

Following the original suggestions of Onsager[37] and Feynman,[38] we shall assume that in a steadily rotating vessel the superfluid component comes into rotation only by virtue of the formation of quantum superfluid vortices. Let us assume that the vortices each have a circulation of h/m_4, where h is Planck's constant, and that they are rectilinear, lying parallel to the axis of rotation. Fetter has shown in a classical calculation that under these circumstances, for a vessel in the form of a right cylinder of arbitrary cross section and connectivity, the equilibrium distribution of vortices is an array of uniform density per unit area $2\omega m_4/h$, where ω is the angular velocity of the vessel.[39] The calculation assumes that ω is large enough so that many vortices are present. As a result, the equilibrium vortex array rotates in solid-body fashion with the vessel, and the local average superfluid velocity is that of solid-body rotation. The normal component of the liquid is assumed to rotate in solid-body fashion like an ordinary viscous fluid.

An individual rectilinear superfluid vortex has associated with it the following irrotational velocity field: Let r, θ, and z be cylindrical coordinates for which the z axis coincides with the vortex core. In terms of these coordinates the velocity lies everywhere in the θ direction and has magnitude $h/2\pi m_4 r$. It seems probable that the density of the superfluid component vanishes at the vortex core. Fetter has considered the case of a vortex in a dilute gas of Bose particles having a short-range repulsive interaction.[40] He finds that in this case the square of the absolute value of the condensate order-parameter is to a reasonable approximation proportional to the expression $r^2/(r^2+a^2)$, where a is some constant. Although it is not known whether it is appropriate to apply this same form to the superfluid density in liquid helium, Parks and Donnelly[11] have used this form to analyze the vortex-ring results of Rayfield and Reif.[41] Their analysis yields a value of a equal to 1.46 ± 0.14 Å. The behavior of the total density ρ near the vortex is still unknown.

C. The Interaction Between Negative Ion and Vortex

In order to discuss the interaction between the negative ion and a vortex we adopt the classical hydrodynamic model developed by Donnelly and co-workers.[10, 11, 42] If a negative-ion bubble is present in the vicinity of a rectilinear vortex at a perpendicular distance r, as shown in Fig. 8 (b), the kinetic energy of the flow around the vortex is lowered. The change in this kinetic energy represents an effective potential energy of interaction $U(r)$ between ion and vortex. Although it does not seem possible to find a closed form for $U(r)$ for all r, there are two limiting cases, $r = 0$ and $r \gg R$, for which $U(r)$ takes a simple form.

For the case $r = 0$, shown in Fig. 8 (a), the velocity field of the vortex is not altered outside the

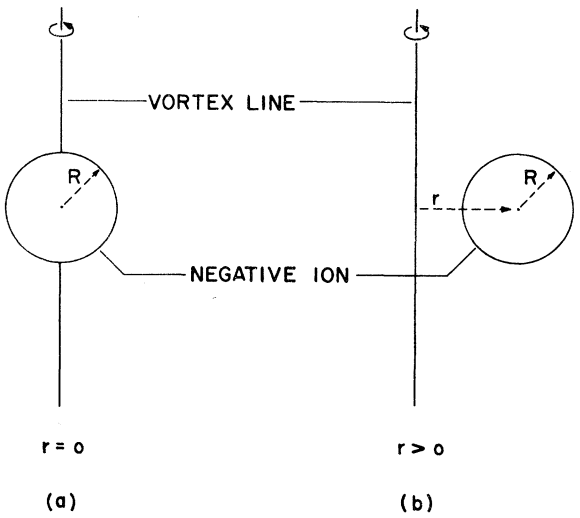

FIG. 8. Sketches of a negative ion situated (a) along and (b) near a vortex line.

ion; and $U(0)$ is just the negative of the kinetic energy that would have been present in a sphere of radius R centered on the vortex were the ion not there. As Parks and Donnelly have shown, $U(0)$ is given by the expression

$$U(0) = -2\pi\rho_s(h/2\pi m_4)^2 K \times\{[1+(a^2/R^2)]^{1/2}\sinh^{-1}(R/a)-1\}, \quad (2)$$

when use is made of the dependence of superfluid density upon r near the vortex described in the preceding subsection. Here ρ_S is the ordinary superfluid density, the density which applies far from the vortex. If we take $R = 19.5$ Å and $a = 1.46$ Å and if we choose $\rho_S = 0.1171$ g cm^{-3}, the value of ρ_S at 1.65°K and saturated vapor pressure, then $U(0)/k$, where k is Boltzmann's constant, equals -60.1°K.

For $r \gg R$, a calculation made long ago by Thomson[43] shows that $U(r)$ is given asymptotically by the expression

$$U(r) \sim -\frac{3}{2}\frac{\rho_S}{2}\left(\frac{h}{2\pi m_4}\right)^2\left(\frac{4\pi R^3}{3}\right)\frac{1}{r^2}. \quad (3)$$

A $1/r^2$ dependence at large r was first proposed for the ion-vortex problem by Donnelly.[10] His estimate of the coefficient of $1/r^2$ as modified in a later publication[42] agrees with the expression above which Thomson derived from first principles.

In considering the problem of the thermally activated escape of the ion from the potential well in the presence of not-too-strong an electric field, it turns out that the only additional feature of $U(r)$ that we need know is the derivative $(d^2U/dr^2)_{r=0}$ at the bottom of the well. Parks and Donnelly have estimated this derivative by assuming that for small values of r, just as for $r = 0$, $U(r)$ is the negative of the kinetic energy that the fluid in the region occupied by the bubble would have had in the absence of the bubble.[11] The result is given by the expression[8]

$$\left(\frac{d^2U}{dr^2}\right)_{r=0} = \pi\rho_S\left(\frac{h}{2\pi m_4}\right)^2\frac{1}{R} \times\frac{\left(2+\frac{a^2}{R^2}\right)\left(1+\frac{a^2}{R^2}\right)^{-1/2}\sinh^{-1}\frac{R}{a}-1}{(1+a^2/R^2)}. \quad (4)$$

While the assumption upon which this formula is based is accurate for $r = 0$, it is not exact for $r > 0$, since it ignores the distortion in the flow pattern around the vortex outside the ion. Furthermore, it seems likely that when r is small but nonzero the vortex line itself will be distorted from rectilinear in the vicinity of the ion. Hence there exists considerable doubt about the accuracy of Eq. (4) as an estimate for $(d^2U/dr^2)_{r=0}$.

In these calculations we have regarded the ion as a hard sphere of radius R and have treated the superfluid flow around it like nonviscous flow of a classical ideal fluid. We have not attempted to consider the actual behavior of the superfluid close to the ion. In particular, we have not considered the possibility that near the ion the superfluid density decreases to zero in some characteristic distance comparable to a. However, it is conceivable that our neglect can be taken care of by assigning to the ion an effective hydrodynamic radius which may differ from the bubble-model radius defined in terms of the electron probability distribution or the density distribution of helium atoms. If so, it is this hydrodynamic radius which is of relevance in the present experiment.

D. The Escape of Negative Ions Bound to Vortex Lines in the Presence of an Electric Field

Let us suppose that a uniform electric field $\vec{\mathcal{E}}$ is present which lies perpendicular to the vortex core. It is convenient now to superimpose upon our cylindrical coordinate system a Cartesian system whose z axis coincides with the previous z axis and whose x axis lies in the direction of the force exerted by $\vec{\mathcal{E}}$ on the ion. The total potential energy of the ion $V(x, y)$ can then be written

$$V(x,y) = U(r) - e\mathcal{E}x, \quad (5)$$

where e is the absolute value of the electronic charge. The form of $V(x, y)$ along the x axis is illustrated in Fig. 9. For $|x| \geq 30$ Å the form for $U(r)$ given by Eq. (3) was used, and for $|x| \leq 7.5$ Å the parabolic form determined by Eqs. (2) and (4) was used. Smooth connections between the two forms were drawn by eye in the intervening regions. In addition to the minimum at $r = 0$, a point we label A, the potential $V(x, y)$

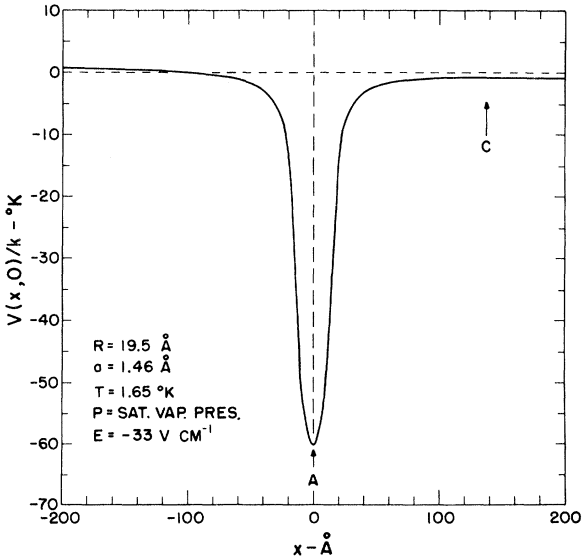

FIG. 9. Total potential energy V of a negative ion in the presence of a vortex located at the origin when a uniform electric field is present perpendicular to the vortex. The x axis lies parallel to the electric field, but runs in the opposite direction. The detailed shape of the interior of the well is rather uncertain.

has a saddle point at a point we label C along the positive x axis; and $V(x, y)$ goes off to $-\infty$ as x goes to $+\infty$. At finite temperatures an ion bound in the potential well can escape over the potential barrier with a mean lifetime τ in the well which we wish to determine.

The escape of the ion has been studied by Donnelly and co-workers.[10,11,42,44] Their treatment is based on the discussion of the escape of a Brownian particle over a potential barrier given by Chandrasekhar.[45] In this treatment an expression for the trapping lifetime is obtained by solving the generalized Fokker-Planck equation. Because in the present case the depth of the well $V(x_C, 0) - V(0, 0)$ is much greater than kT and because the coefficient of friction $\beta \equiv e/m_i\mu$, where μ is the ion mobility, is much greater than

$$\omega_{Cx} \equiv \left[-\frac{1}{m_i}\left(\frac{\partial^2 V}{\partial x^2}\right)_C\right]^{1/2}$$

throughout the region of temperature and pressure studied, the solution also satisfies the simpler time-independent Smoluchowski equation. It is shown that in this case the trapping lifetime is given by the approximate expression

$$\tau \approx \frac{2\pi e}{\mu}\frac{1}{m_i\omega_{Ax}\omega_{Ay}}\frac{\omega_{Cy}}{\omega_{Cx}}\exp\left(\frac{V_C - V_A}{kT}\right), \tag{6}$$

where

$$\omega_{Ax}^2 \equiv \frac{1}{m_i}\left(\frac{\partial^2 V}{\partial x^2}\right)_A, \quad \omega_{Ay}^2 \equiv \frac{1}{m_i}\left(\frac{\partial^2 V}{\partial y^2}\right)_A,$$
$$\omega_{Cx}^2 \equiv -\frac{1}{m_i}\left(\frac{\partial^2 V}{\partial x^2}\right)_C, \quad \omega_{Cy}^2 \equiv \frac{1}{m_i}\left(\frac{\partial^2 V}{\partial y^2}\right)_C, \tag{7}$$

and where $V_A \equiv V(0, 0)$ and $V_C \equiv V(x_C, 0)$.

Making use of Eq. (5) and the expressions for $U(r)$ developed in the preceding subsection we have the following formulas for the quantities which appear in the expression for τ given above:

$$\omega_{Ax}^2 = \omega_{Ay}^2 \approx \frac{\pi\rho_s}{m_i}\left(\frac{h}{2\pi m_4}\right)^2\frac{1}{R} \times \frac{\left(2+\frac{a^2}{R^2}\right)\left(1+\frac{a^2}{R^2}\right)^{-1/2}\sinh^{-1}\frac{R}{a} - 1}{(1+a^2/R^2)}, \tag{8}$$

$$\omega_{Cy}^2/\omega_{Cx}^2 \approx \tfrac{1}{3}, \tag{9}$$

$$V_A \approx -2\pi\rho_s(h/2\pi m_4)^2 R \times[(1+a^2/R^2)^{1/2}\sinh^{-1}(R/a) - 1], \tag{10}$$

$$V_C \approx -\tfrac{3}{2}(2\pi)^{1/3}(h/2\pi m_4)^{2/3}\rho_s^{1/3}e^{2/3}\mathcal{G}^{2/3}R. \tag{11}$$

In writing Eqs. (9) and (11) use has been made of the fact that for the electric field strengths employed, the saddle point C is expected to be well into the asymptotic region $r \gg R$ where Eq. (3) for $U(r)$ is thought to be a good approximation.

In the following section of the paper we shall attempt to fit our experimental lifetime results using Eq. (6) in connection with Eqs. (8) through (11). In so doing we will attempt to determine an effective ion radius R as a function of pressure, assuming that it is independent of temperature at any given pressure. In order to do this it is helpful to rewrite Eq. (6) for τ in a form which displays explicitly its dependence on temperature, pressure, and ion radius. We may rewrite our expressions for $\omega_{Ax}^2 = \omega_{Ay}^2$, V_A, and V_C in the forms

$$\omega_{Ax}^2 = \omega_{Ay}^2 \approx [\rho_s(T,P)/\rho_{s0}]\,\omega_{A0}^2(R), \tag{12}$$

$$V_A \approx [\rho_s(T,P)/\rho_{s0}]\,V_{A0}(R), \tag{13}$$

$$V_C \approx [\rho_s(T,P)/\rho_{s0}]^{1/3}V_{C0}(R), \tag{14}$$

where the subscript 0 denotes some convenient common fixed reference temperature and pressure at which the quantities so labeled are to be evaluated. Then τ may be written

$$\tau(T,P,R) \approx \frac{2\pi e}{\sqrt{3}}\frac{1}{\mu(T,P)}\frac{\rho_{s0}}{\rho_s(T,P)}\frac{1}{m_i(R)\omega_{A0}^2(R)} \times\exp\left\{\frac{1}{kT}\left[\left(\frac{\rho_s(T,P)}{\rho_{s0}}\right)^{1/3}V_{C0}(R) - \frac{\rho_s(T,P)}{\rho_{s0}}V_{A0}(R)\right]\right\}. \tag{15}$$

VI. INTERPRETATION OF THE RESULTS

A. Preliminaries

We now wish to compare the predictions of the theory of the preceding section with our lifetime results and to determine values for the ion radius at the various pressures at which measurements were made. In order to fit Eq. (15) to the data it is necessary to know the functions $\mu(T, P)$ and $\rho_s(T, P)$ in the region of measurement.

The mobility of the negative ion has been measured by several investigators.[8,46-48] We have used the following expression to approximate their results for the purpose at hand,

$$\mu(T,P) \approx \mu_\infty \exp[\Delta(P)/T], \tag{16}$$

where

$$\Delta(P) = 8.10°\text{K}, \quad 0 \leq P \leq 5\text{ atm},$$
$$= 8.37°\text{K} - (0.055°\text{K atm}^{-1})P, \quad 5\text{ atm} \leq P \leq 25\text{ atm},$$

and where $\mu_\infty = 1.2\times10^{-3}\,\mathrm{cm^2\,sec^{-1}\,V^{-1}}$.

With this approximation it is convenient for the following analysis to rewrite Eq. (15) in the form

$$\tau \approx \tau_0 \exp\left\{-\ln\frac{\rho_s}{\rho_{s0}} + \frac{1}{T}\left[-\Delta+\left(\frac{\rho_s}{\rho_{s0}}\right)^{1/3}\frac{V_{C0}}{k}-\frac{\rho_s}{\rho_{s0}}\frac{V_{A0}}{k}\right]\right\}, \quad (17)$$

where

$$\tau_0(R) \equiv 2\pi e/\sqrt{3}\;\mu_\infty m_i(R)\omega_{A0}{}^2(R). \quad (18)$$

Our assumptions regarding $\rho_S(T,P)$ are discussed in the following subsections.

B. Results at Saturated Vapor Pressure

At saturated vapor pressure a computer-calculated fit was made of Eq. (17) to the data taken with $Vg = -40$ V making use of the following assumptions and approximations. Keeping in mind that the data at this pressure lie between the temperatures of 1.590 and 1.680°K, it is convenient here to choose the reference temperature and pressure in Eqs. (17) and (18) to be 1.650°K and saturated vapor pressure, respectively. With this choice the quantity V_{C0} appearing in the exponent of Eq. (17) was expected to be very much smaller in magnitude than V_{A0}. Under these circumstances it proved easier in fitting Eq. (17) to the data to replace the quantity

$$(\rho_s/\rho_{s0})^{1/3}\,V_{C0}/k - (\rho_s/\rho_{s0})V_{A0}/k$$

in the exponent by the quantity $(\rho_S/\rho_{S0})\,\Delta V_0/k$, where $\Delta V \equiv V_C - V_A$. The error introduced by this substitution can be corrected at the end of the calculation and will be described below. Equation (17) then takes the approximate form

$$\tau \approx \tau_0' \exp\left\{-\ln\frac{\rho_s}{\rho_{s0}} + \frac{1}{T}\left[-\Delta+\frac{\rho_s}{\rho_{s0}}\frac{\Delta V_0'}{k}\right]\right\}, \quad (19)$$

where the primes attached to τ_0 and ΔV_0 are intended to remind us of the approximation involved in using Eq. (19) instead of Eq. (17).

The form of $\rho_S(T)$ at saturated vapor pressure was chosen as follows, using the relation $\rho_S = \rho - \rho_n$, where ρ_n is the density of the normal fluid component. The form of ρ was determined by interpolation of the data of Kerr and Taylor[49] and was taken to be

$$\rho(T) = 0.1462\ \mathrm{gm\,cm^{-3}} - (0.0016\ \mathrm{g\,cm^{-3}\,^\circ K})\frac{1}{T}. \quad (20)$$

The form of $\rho_n(T)$ was taken to be

$$\rho_n(T) = (8.75\ \mathrm{g\,cm^{-3}})\exp(-9.47\,^\circ\mathrm{K}/T), \quad (21)$$

which in the temperature region of interest fits well the values of ρ_n calculated from second sound velocities and other thermodynamic data by Hussey *et al.*[50]

With these assumptions Eq. (19) was fitted to the $V_g = -40$ V data using the method of least squares, treating $\tau_0'(R)$ and $\Delta V_0'(R)/k$ as free parameters. The resulting function is shown in Fig. 4 as the curve which passes through the $V_g = -40$ V points. The other curves are merely parallel displacements of this first curve upwards and downwards. The resulting values for $\tau_0'(R)$ and $\Delta V_0'(R)/k$ are given by the expressions

$$\tau_0'(R) = (1.5\pm0.2)10^{-12}\ \mathrm{sec}, \quad (22)$$

$$\Delta V_0'(R)/k = (59.4\pm0.2)^\circ\mathrm{K}. \quad (23)$$

The value of $\Delta V_0'(R)/k$ is in effect determined by the derivative $d(\ln\tau)/d(1/T)$. At first glance, then, it may seem strange that the slope of the curve in Fig. 4 determined by computer, a slope of approximately 131°K, should be so much larger than the value of $\Delta V_0'(R)/k - \Delta$, which is approximately 51°K. The quantity $\Delta V_0'(R)/k - \Delta$ is the coefficient of $1/T$ in the exponent of Eq. (19) at 1.650°K, and the entire temperature dependence of τ is carried in this exponent. However, the large difference arises mainly from the fact that ΔV is itself a temperature-dependent quantity, owing to the temperature dependence of $\rho_S(T)$. Because such a large difference arises from a rather small variation in ρ_S over the region of interest, the value of $\Delta V_0'(R)/k$ determined by computer fit is quite sensitive to the temperature dependence assumed for $\rho_S(T)$. It is further worth noting that if some relatively small additional temperature dependence in ΔV should be included in the model, for example a dependence of ion radius R on T, the change in the value of $\Delta V_0'(R)/k$ resulting might be relatively large.

We now have at our disposal values for two radius-dependent parameters $\tau_0'(R)$ and $\Delta V_0'(R)/k$. In principle, a value for R could be determined from either of them. However, because $\tau_0(R)$ is inversely proportional to $(d^2U/dr^2)_A$ for which we may not have an accurate estimate, we choose to determine R from $\Delta V_0'(R)/k$. Using Eqs. (10), (11), (13), and (14), assuming length a to have the value 1.46 ± 0.14 Å, and taking $\mathcal{E}$ to be the average value 33.2 V cm^{-1}, we compute the ion radius at saturated vapor pressure to be

$$R = 19.5\pm0.6\ \text{Å}. \quad (24)$$

Most of the uncertainty assigned comes from the uncertainty assumed for the length a.

At this point we can estimate the error introduced on approximating Eq. (17) by Eq. (19). With the correct dependence of V_C on (ρ_S/ρ_{S0}) we obtain the corrected values

$$\tau_0(R) = (1.8\pm0.2)10^{-12}\ \mathrm{sec}, \quad (25)$$

$$\Delta V_0(R)/k = (59.1\pm0.2)^\circ\mathrm{K}. \quad (26)$$

The value of R computed from $\Delta V_0/k$ does not differ significantly from the value given above.

However, a serious inconsistency exists between the model and our experimental results. For if we use the value of R above to compute from the model the value of $\tau_0(R)$ expected using Eqs. (8), (12), and (18), we obtain the result $\tau_0(R) = (1.8)10^{-8}$ sec, a value four orders of magnitude larger than that obtained above by fitting the data!

Because the estimate given by Eq. (4) for $(d^2U/dr^2)_A$ at the bottom of the well is open to considerable question, it is tempting to try to remove the discrepancy by modifying the shape of the bottom of the well. However, a decrease in τ_0 by a factor of 10^4 would correspond to a reduction of the radial scale of the well bottom by a factor of 10^2, ignoring the importance of whatever quantum corrections to the classical theory of escape would be required due to the increase in ω_A^2. Such a large reduction is hard to explain.

Another possible source of the discrepancy in $\tau_0(R)$ may lie in the shallowness of the lip of the potential at C. It may be seen in Fig. 9 that under representative conditions V_C is roughly a factor of two smaller than kT. Under these circumstances it is doubtful that the approximations used near point C in integrating the Smoluchowski equation to derive Eq. (6) are very accurate. However, it is unlikely that this effect would account for a major part of the total discrepancy.

Thus one is faced with at least a partial breakdown of the model, and one cannot reasonably use the model as it stands to fit both the magnitude of the lifetime and its temperature dependence at the same time. As is implicit in the discussion above we have chosen to regard the temperature dependence as the most significant aspect to fit, and in so doing we have arrived at the radius stated above. On the other hand, Parks and Donnelly,[11,42] in their earlier analysis of Douglass's results,[3] chose to fit the magnitude rather than the temperature dependence and arrived at the somewhat smaller radius of 16.0Å. Because of the discrepancy between model and experiment, both determinations of the radius must be viewed with considerable reservation.

It is of interest to note that an experimental determination of the negative-ion radius at saturated vapor pressure employing an entirely different method has recently been made by Northby and Sanders.[51] In their experiment the ion radius was determined from studies of the photoejection of the electron from the bubble and was found to be 21.2 ± 0.5Å.

Let us now consider several effects which may have caused our experimental lifetimes to differ from the true lifetimes. In so doing it is useful to consider the electric-field dependence of the lifetime. According to our models the true lifetime is field dependent because of the field dependence of V_C and hence of the effective well depth. According to Eqs. (6) and (11), τ depends on $\mathcal{E}$ through the factor $\exp(V_C/kT)$ in which V_C is proportional to $\mathcal{E}^{2/3}$.[3] This field dependence at 1.65°K and saturated vapor pressure is shown in relative units by curve A in Fig. 5. It may be seen that this field dependence does not give an accurate account of the field dependence observed.

The steep rise in the lifetime observed at low fields is thought to be due to ion recapture after escape. A simple model for the decay of the charge distribution taking recapture into account was constructed assuming a uniform vortex-line density, a uniform initial charge distribution, and using the field-dependent capture widths reported by Tanner[5] extrapolated to field values below 10 V cm^{-1}. A uniform electric field and lifetime for single escape were assumed. The decay of charge computed from this model is very nearly exponential, with an effective lifetime which differs from the true lifetime for single escape by a factor which is field dependent. Curve B in Fig. 5 represents the result of multiplying curve A by this factor and thus shows in relative units the resulting effective lifetime as a function of electric field. Curve B is seen to give a considerably better account of the field dependence observed than curve A. It is clear that recapture effects are particularly important at low field values. At $\mathcal{E} = 33.2$ V cm^{-1} recapture is estimated to cause the effective lifetime to be a factor of about 1.04 larger than the true lifetime for single escape.

The effect of including recapture effects in fitting Eq. (17) to the data would not be great. Because the correction due to recapture is thought to be a rather slowly varying function of temperature over the temperature range of interest at saturated vapor pressure, the principal result of including this correction would be to decrease the value of $\tau_0(R)$ by a small amount while leaving $\Delta V_0(R)/k$ unchanged. Hence the inclusion of recapture effects would not shift significantly the value that we have determined for R.

Because recapture effects are dependent on the vortex-line density, they can give rise to a small dependence of lifetime on rotation speed. Such a cause is adequate to account for the small dependence of lifetime on rotation speed that was observed.

Another effect to be considered arises from the fact that the field was nonuniform between the gate and collector. Because the lifetime is field dependent, the observed decay was in fact a composite of decays of different lifetime. The make-up of this composite was dependent on the initial charge distribution between the gate and collector. However, equal amounts of charge at different radial locations between the gate and collector did not contribute equally. Because the amount of charge induced on the collector by a given amount of trapped charge depended on the location of the trapped charge, so also did the amount of apparent charge arising from that charge depend on its location.

Calculations were made of the composite decay expected at 1.65°K and saturated vapor pressure assuming a uniform initial distribution of charge and a dependence of lifetime on field given by curve A in Fig. 5. The resulting decay is quite exponential over periods of at least two lifetimes. The effective lifetime differs from the lifetime of curve A evaluated at $\mathcal{E}_{av}$ by a field-dependent factor which equals 0.94 at $\mathcal{E} = 33.2$ V cm^{-1}. Curve C in Fig. 5 represents the result of multi-

plying curve A by this factor and thus shows in relative units the field dependence of the effective lifetime resulting when field-nonuniformity (but not ion-recapture) effects are included.

The calculations indicate that at $\mathcal{E}_{av} = 33.2$ V cm^{-1} the correction to the lifetime due to field nonuniformity at saturated vapor pressure is rather independent of temperature. Thus the inclusion of this correction in fitting Eq. (17) to the data would increase $\tau_0(R)$ by a small amount while leaving $\Delta V_0(R)/k$ and R essentially unaffected.

It is plausible from Fig. 5 that if the recapture corrections leading to curve B and the field-nonuniformity corrections leading to curve C were simultaneously taken into account in a consistent way, the resulting field dependence of the lifetime would agree rather well with the field dependence observed.

C. Results at Elevated Pressure

In order to fit Eq. (17) to the lifetime results at elevated pressure and to determine values for the ion radius at these pressures, two procedures were used. Values of $\rho_S(T,P)$ required for both these procedures were obtained from calculations of $\rho_n(T, P)$ using the relation $\rho_S = \rho - \rho_n$. The total density ρ was taken from Boghosian and Meyer[52] and Elwell and Meyer.[53] For temperatures between 1.10 and 1.30°K, $\rho_n(T, P)$ was taken from the calculations of Boghosian and Meyer.[52] For temperatures between 1.20 and 1.65°K, $\rho_n(T, P)$ was calculated from second sound velocities and other thermodynamic data using the relation

$$\rho_n = \rho / [1 + (u_2{}^2 C_V / S^2 T)] .$$

The second sound velocity $u_2{}^2$ was taken from Maurer and Herlin.[54] The specific heat at constant volume C_V was taken from Lounasmaa,[55] and the entropy S from van den Meijdenberg *et al.*[56]

At each pressure for which lifetime measurements were made, $\ln\rho_n$ was plotted versus $1/T$. At all pressures these plots yielded rather straight lines. In the region of overlap between 1.20 and 1.30°K the agreement between the two sets of ρ_n values was reasonably good. Using these plots of ρ_n, ρ_S could be determined as a function of T at each pressure. In particular, ρ_S was determined along the curves of constant lifetime, and these values are listed in Table IV.

The first procedure used for determining the ion radius at elevated pressure was to follow along a curve of constant lifetime, using Eq. (17), in which $\tau_0(R)$ was regarded as a fixed constant given by Eq. (25), to compute a value of R at each value of the pressure. The length a characterizing the size of the vortex core was also taken to be a constant equal to the value 1.46 Å used at saturated vapor pressure. Calculations were carried out by this method along each of the three curves of constant lifetime, and the three values of R determined at each pressure were averaged. These averages are shown plotted as solid circles in Fig. 10. At each pressure the agreement between the three values of R was quite good. In each case the range of values was less than 0.2 Å, a magnitude comparable to the diameter of the circles in Fig. 10.

Because of the discrepancy between the value of $\tau_0(R)$ given by Eqs. (8), (12), and (18) and that given by Eq. (25), our procedure here is open to the same questions that applied at saturated vapor pressure. In addition, our treatment of $\tau_0(R)$ as a fixed constant can be questioned. Fortunately, the values of R determined in these calculations are fairly insensitive to variations in $\tau_0(R)$. For example, according to the development of Sec. V, $\tau_0(R)$ given by Eqs. (8), (12), and (18) should vary with R approximately in proportion to R. If we assume that this same variation applies to the $\tau_0(R)$ we have used, our value of R at 24 atm would be increased by only 0.1 Å.

The treatment of length a as a constant is also open to question. Little is known about how this quantity might depend on pressure. In Fetter's

TABLE IV. Superfluid density ρ_S calculated from thermodynamic data for points along the curves of constant lifetime.

	τ=20 sec		τ=85 sec		τ=350 sec	
P (atm)	T (°K)	ρ_S (g cm^{-3})	T (°K)	ρ_S (g cm^{-3})	T (°K)	ρ_S (g cm^{-3})
0.0	1.669	0.1152	1.642	0.1180	1.610	0.1208
1.0	1.606	0.1222	1.575	0.1252	1.545	0.1276
2.0	1.562	0.1273	1.528	0.1296	1.498	0.1316
3.0	1.522	0.1308	1.489	0.1329	1.458	0.1348
4.0	1.486	0.1338	1.452	0.1360	1.421	0.1379
5.0	1.458	0.1361	1.422	0.1383	1.389	0.1402
6.0	1.432	0.1385	1.395	0.1406	1.362	0.1424
8.0	1.381	0.1427	1.345	0.1446	1.312	0.1463
10.0	1.338	0.1461	1.304	0.1480	1.271	0.1495
12.0	1.300	0.1492	1.266	0.1510	1.234	0.1524
14.0	1.264	0.1520	1.231	0.1535	1.201	0.1549
16.0	1.232	0.1545	1.200	0.1559	1.170	0.1573
18.0	1.205	0.1567	1.173	0.1580	1.143	0.1594
20.0	1.179	0.1587	1.147	0.1600	1.117	0.1614
22.0	1.151	0.1607	1.121	0.1619	1.092	0.1632
24.0	1.129	0.1621	1.097	0.1636		

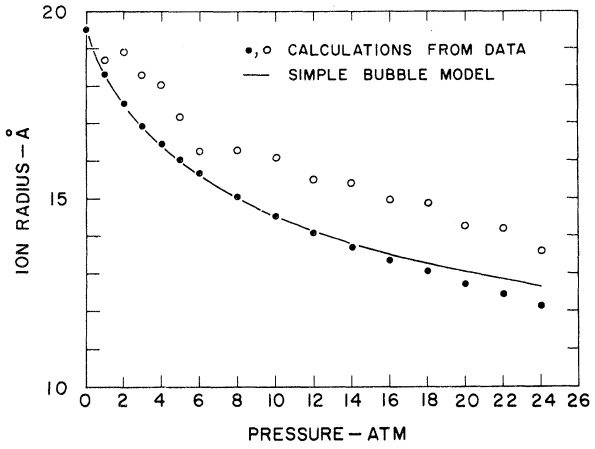

FIG. 10. Ion radius as a function of pressure. The solid circles show our results using the first method of analysis, the open circles our results using the second method. The curve shows the prediction of the simple bubble model with σ adjusted to give $R = 19.5$ Å at $P = 0$.

calculations for a dilute gas of interacting Bose particles,[40] the length characterizing the size of the vortex core is proportional to $\rho^{-\frac{1}{2}}$. If such a dependence is applied in these calculations, our value of R at 24 atm should be reduced by 0.4 Å.

The second procedure used for determining the ion radius at elevated pressure was to apply at each pressure essentially the same method used at saturated vapor pressure in somewhat simplified form. Because in this method the value of $\Delta V_0(R)/k$ and hence that of R can be determined from the slope of $\ln\tau$ versus $1/T$, the values of $d(\ln\tau)/d(1/T)$ given in Table II and plotted in Fig. 6 may be regarded as the basis for these calculations. The results of these calculations are shown by the open circles in Fig. 10. Some sort of major discrepancy exists between these results and the results of the first procedure. Not only do these points depart from those of the first procedure, but they also show more scatter.

We suspect that the second procedure is less reliable than the first at elevated pressure because it is considerably more sensitive to small errors in our assumptions regarding the dependence of ρ_S on T. It remains unclear whether the change in slope at 6 atm that appears in Fig. 6 really reflects a change in the slope of $R(P)$ at that same pressure, as the open circles in Fig. 10 suggest, or whether it is due to some other cause.

The curve in Fig. 10 shows the form of $R(P)$ obtained by the simple bubble-model calculation of Sec. V with σ adjusted to the value 0.332 erg cm^{-2} in order to make $R(0)$ agree with the value of 19.5 Å obtained from the data. The remarkable agreement between the pressure dependence of R calculated from the model and that resulting from the first method of analysis of the data must not be taken too seriously, in view of the simplicity of the bubble-model calculation.

Although we have not tried to make a detailed comparison, the general shape of the dependence of R on P given by the solid circles compares favorably with the shape of the dependence determined by Springett and Donnelly from capture width measurements.[7,8] Their analysis, however, is based on the assumption that the ion radius at saturated vapor pressure is 16.0 Å.

On the basis of a similar analysis, our failure to observe positive-ion trapping at 1.095°K at the solidification pressure means that the effective radius of the positive ion is probably less than 12 or 13 Å at this pressure.

VII. DISCUSSION AND CONCLUDING REMARKS

In the preceding sections we have described the results of our lifetime measurements and have interpreted them in terms of models of the ion and of the rotating liquid. We have tried to make a clear division between the experimental results and their interpretation, because of a number of questions and difficulties which arise in the interpretation. The experimental data may well bear re-analysis as the models and the supplementary data needed in the analysis are improved.

In regard to the experiment itself, the use of cylindrical geometry, in which the electric field was not uniform, was less than ideal because of the field dependence of the lifetime being studied. A parallel-plate uniform-field geometry would seem more suitable. However, the discussion given in the preceding section indicates that the range of field values present probably did not introduce serious difficulties into our interpretation of the data. Furthermore, cylindrical geometry has the advantage that less disturbance is produced in the liquid when rotation is started or stopped. We chose cylindrical geometry at a stage in the experiment when we expected to be investigating the starting and stopping of rotation in more detail.

The principal difficulties encountered in the interpretation of the data are the following. First, considerable uncertainty exists in regard to the details of the model for the ion-vortex interaction when the two are near to each other. Among the questions which arise are those concerning the behavior of ρ_S and ρ near the vortex, the role of distortions and possibly vibrations of the vortex line, and the applicability of the hydrodynamic model. It seems possible, for example, that if the total fluid density ρ varies near the core of a vortex there may be other than hydrodynamic contributions to the ion-vortex interaction.

Second, it has proved impossible to fit both the magnitude and the slope of $\ln\tau$ versus $1/T$ using the models discussed in Sec. V as they stand. If the ion radius is chosen so that the slopes agree, the magnitude of τ determined from the models is much larger than that observed. Third, the two methods of analyzing the data at elevated pressure yield rather discrepant results.

It is quite likely that all of these difficulties are closely related. However, a major part of the last may be due to inaccuracies in our assumptions regarding $\rho_S(T, P)$. It may be that a more accurate determination of $\rho_S(T, P)$ can be made using existing data. However, it seems that it would be quite desirable to have more accurate thermodynamic data from which $\rho_S(T, P)$ could be deter-

mined. It would be particularly desirable to have direct measurements of $\rho_s(T, P)$ using the gyroscopic technique[57, 58] or of $\rho_n(T, P)$ using the Andronikashvili method.[59]

The spirit of the present interpretation has been to assume a knowledge of the vortex nature of rotating superfluid helium and of the ion-vortex interaction and to derive values for the ion radius from the data. Because of the problems mentioned above this attempt has had only qualified success. It may be that in the future the more appropriate procedure will be to make use of values of $R(P)$ determined in some experiment quite independent of rotation, such as the electron photoejection experiment of Northby and Sanders,[51] and to use the trapping-lifetime experiments to give information about the ion-vortex interaction.

VIII. ACKNOWLEDGMENTS

The authors would like to acknowledge the support given this work by the U.S. Atomic Energy Commission.[60] Thanks are due to Dr. R. Stryk for making available his computer program for the least-squares analysis used in interpreting the data. One of us (W.P.P.) would like to acknowledge the tenure of a National Aeronautics and Space Administration fellowship during part of this work and the support of the Los Alamos Scientific Laboratory of the University of California during the final preparation of this report. The other (W.Z.) would like to acknowledge the tenure of a National Science Foundation Senior Postdoctoral Fellowship and the hospitality of the Department of Technical Physics of the Technical University of Helsinki during the final preparation of this report.

---

*Present address: Los Alamos Scientific Laboratory, Los Alamos, New Mexico.

[1]G. Careri, W. D. McCormick, and F. Scaramuzzi, Phys. Letters 1, 61 (1962).
[2]D. J. Tanner, B. E. Springett, and R. J. Donnelly, in Proceedings of the Ninth International Conference on Low Temperature Physics, edited by J. G. Daunt, D. O. Edwards, F. J. Milford, and M. Yaqub (Plenum Press, Inc., New York, 1965), p. 346.
[3]R. L. Douglass, Phys. Rev. Letters 13, 791 (1964).
[4]B. E. Springett, D. J. Tanner, and R. J. Donnelly, Phys. Rev. Letters 14, 585 (1965).
[5]D. J. Tanner, Phys. Rev. 152, 121 (1966).
[6]R. L. Douglass, Phys. Rev. 141, 192 (1966).
[7]B. E. Springett and R. J. Donnelly, Phys. Rev. Letters 17, 364 (1966).
[8]B. E. Springett, Phys. Rev. 155, 139 (1967).
[9]A detailed account of the present work has been given by W. P. Pratt, Jr., Ph.D. thesis, University of Minnesota, 1967 (unpublished).
[10]R. J. Donnelly, Phys. Rev. Letters 14, 39 (1965).
[11]P. E. Parks and R. J. Donnelly, Phys. Rev. Letters 16, 45 (1966).
[12]Microsphere source, Nuclear Products Division, Minnesota Mining and Manufacturing Co., St. Paul, Minn.
[13]ADVAC Products, Inc., Stamford, Conn.
[14]Epibond 100 A, Furane Plastics, Inc., Los Angeles, Calif.
[15]Model 55354S, National Seal Division, Federal-Mogul-Bower Bearings, Inc., Detroit, Mich.
[16]Model N30VM, Graham Transmissions, Inc., Menomonee Falls, Wisc.
[17]Series 1400, U.S. Gauge Division, American Machine and Metals, Inc., Sellersville, Pa.
[18]C. Blake and C. E. Chase, Rev. Sci. Instr. 34, 984 (1963).
[19]Cryoresistor S/N 42, Cryocal, Inc., Riviera Beach, Florida.
[20]F. G. Brickwedde, H. van Dijk, M. Durieux, J. R. Clement, and J. K. Logan, The "1958 He^4 Scale of Temperatures," National Bureau of Standards Monograph 10 (U. S. Government Printing Office, Washington, D. C., 1960).
[21]Consolidated Vacuum Corp., Rochester, N.Y.
[22]T. R. Roberts and S. G. Sydoriak, Phys. Rev. 102, 304 (1956).
[23]R. L. Douglass, private communication. Douglass's lifetime measurements were made using an inner radius of 0.375 cm, an outer radius of 1.71 cm, and a voltage difference between the conductors of 36 V.
[24]G. Careri, in Progress in Low Temperature Physics, edited by C. J. Gorter (North-Holland Publishing Co., Amsterdam, 1961), Vol. III, Chap. II.
[25]R. A. Ferrell, Phys. Rev. 108, 167 (1957).
[26]C.G. Kuper, Phys. Rev. 122, 1007 (1961).
[27]R. C. Clark, Phys. Letters 16, 42 (1965).
[28]J. Jortner, N. R. Kestner, S. A. Rice, and M. H. Cohen, J. Chem. Phys. 43, 2614 (1965).
[29]K. Hiroike, N. R. Kestner, S. A. Rice, and J. Jortner, J. Chem. Phys. 43, 2625 (1965).
[30]J. L. Levine and T. M. Sanders, Jr., Phys. Rev. 154, 138 (1967).
[31]A. D. Singh, private communication.
[32]B. E. Springett, M. H. Cohen, and J. Jortner, Phys. Rev. 159, 183 (1967).
[33]B. Burdick, Phys. Rev. Letters 14, 11 (1965).
[34]W. T. Sommer, Phys. Rev. Letters 12, 271 (1964).
[35]M. A. Woolf and G. W. Rayfield, Phys. Rev. Letters 15, 235 (1965).
[36]K. R. Atkins and Y. Narahara, Phys. Rev. 138, A437 (1965).
[37]L. Onsager, Nuovo Cimento Suppl. 2 6, 249 (1949).
[38]R. P. Feynman, in Progress in Low Temperature Physics, edited by C. J. Gorter (North-Holland Publishing Co., Amsterdam, 1955), Vol. I, Chap. II.
[39]A. L. Fetter, Phys. Rev. 152, 183 (1966).
[40]A. L. Fetter, Phys. Rev. 138, A429 (1965).
[41]G. W. Rayfield and F. Reif, Phys. Rev. 136, A1194 (1964).
[42]R. J. Donnelly, Experimental Superfluidity (University of Chicago Press, 1967), Chap. 6.
[43]W. Thomson, Phil. Mag. 45, 332 (1873). A presentation of Thomson's derivation in modern notation may be found in Ref. 9.
[44]R. J. Donnelly and P. H. Roberts, unpublished.
[45]S. Chandrasekhar, Rev. Mod. Phys. 15, 1 (1943).
[46]F. Reif and L. Meyer, Phys. Rev. 119, 1164 (1960).
[47]L. Meyer and F. Reif, Phys. Rev. 123, 727 (1961).
[48]S. Cunsolo and P. Mazzoldi, Nuovo Cimento 20, 949 (1961).
[49]E. C. Kerr and R. D. Taylor, Ann. Phys. (N.Y.) 26, 292 (1964).
[50]R. G. Hussey, B. J. Good, and J. M. Reynolds, Phys. Fluids 10, 89 (1967).
[51]J. A. Northby and T. M. Sanders, Jr., Phys. Rev. Letters 18, 1184 (1967).
[52]C. Boghosian and H. Meyer, Phys. Rev. 152, 200 (1966).

[53]D. L. Elwell and H. Meyer, Phys. Rev. 164, 245 (1967).
[54]R. D. Maurer and M. A. Herlin, Phys. Rev. 81, 444 (1951).
[55]O. V. Lounasmaa, Cryogenics 1, 212 (1961).
[56]C. J. N. van den Meijdenberg, K. W. Taconis, and R. de Bruyn Ouboter, Physica 27, 197 (1961).
[57]J. D. Reppy, Phys. Rev. Letters 14, 733 (1965).
[58]J. B. Mehl and W. Zimmermann, Jr., Phys. Rev. Letters 14, 815 (1965); Phys. Rev. 167, 214 (1968).
[59]E. L. Andronikashvili, J. Phys. (USSR) 10, 201 (1946).
[60]Contract No. AT(11-1)-1569. This report is designated COO-1569-26.

Comments and Addenda

The Comments and Addenda section is for short communications which are not of such urgency as to justify publication in Physical Review Letters and are not appropriate for regular Articles. It includes only the following types of communications: (1) comments on papers previously published in The Physical Review or Physical Review Letters; (2) addenda to papers previously published in The Physical Review or Physical Review Letters, in which the additional information can be presented without the need for writing a complete article. Manuscripts intended for this section may be accompanied by a brief abstract for information-retrieval purposes. Accepted manuscripts will follow the same publication schedule as articles in this journal, and galleys will be sent to authors.

PHYSICAL REVIEW VOLUME 177, NUMBER 1 5 JANUARY 1969

Asymptotic Forms for Correlation Functions*

Gerald L. Jones and Vincent P. Coletta
Department of Physics, University of Notre Dame, Notre Dame, Indiana
(Received 29 July 1968)

The range of validity of a general argument for the asymptotic form of correlation functions, presented in a previous paper, is discussed in some detail. The asymptotic form of correlation functions of local variables for one-dimensional lattice and continuous systems are discussed and found to have the predicted form.

I. INTRODUCTION

In a previous paper[1] (hereafter I) a plausible general argument was given for a certain asymptotic form for the correlation function of two local dynamical variables. It was argued that if $A(\vec{r})$ and $B(\vec{r})$ are local dynamical variables and ω stands for the variables specifying the thermodynamic state of the system then for ω near the critical point ω_c and r large enough

$$\langle A(\vec{r})B(0)\rangle - \langle A(\vec{r})\rangle\langle B(0)\rangle \simeq d_A(\omega)d_B(\omega)e^{-\kappa(\omega)r}/r^{b(\omega)}, \quad (1\text{-}1)$$

where $\langle\cdots\rangle$ is the usual average over an equilibrium ensemble. The functions $\kappa(\omega)$ and $b(\omega)$ are the same for a large class of A and B and $\kappa(\omega)\to 0, b(\omega)\to b\geq 0$ as $\omega\to\omega_c$. Near the critical point and for external field equal to zero the spin-spin, spin-energy density and energy-density-energy-density correlation functions of the two dimensional square spin-$\frac{1}{2}$ Ising model are known[2] and have been shown[1] to satisfy Eq. (1-1) for $T<T_c$ (the critical temperature). One might still argue that (1-1) is not a general property of systems in thermal equilibrium, but rather depends on some special properties of the example given. In particular it might depend on: (a) the system being two dimensional, (b) the nearest-neighbor interaction, (c) the system being spin $\frac{1}{2}$, (d) the fact that the external field was zero, (e) the particular choices of dynamical variables $A(\vec{r})$ and $B(\vec{r})$, and (f) the system being a lattice rather than a continuous system. Points (d) and (e) fall under the general question: For what class of variables $A(\vec{r})$, $B(\vec{r})$ and what thermodynamic states ω is (1-1) true? This question is discussed in general in Sec. II.

In Sec. III we discuss the asymptotic form of